

Synthesis and characterization of Titanium Dioxide modified zeolite-x based composite: To study the solar cell application

Ramkumar Singh Dandolia^{1,*}, Shatrughan Singh Tomar², Arvind Dandotia¹, Radha Tomar³,
Rajendra K. Tiwari¹

¹ School of Studies in Physics, Jiwaji University, Gwalior-474011, India

² Govt. SLP PG College, Morar, Gwalior-474006, India

³ School of Studies in Chemistry, Jiwaji University, Gwalior-474011, India

Received 28 April 2022;

revised 06 June 2022;

accepted 14 June 2022;

available online 18 June 2022

Abstract

This paper focuses on the performance of introducing zeolite nanocomposite into photoanodes of dye-sensitized solar cells. Mesoporous titanium dioxide and zeolite nanoparticles were synthesized using hydrothermal technique. The Synthesized nanocomposite was characterized by various techniques via X-ray diffraction technique, Scanning electron microscopy, and Ultraviolet visible spectrophotometer. XRD analysis showed highly crystalline zeolite, Titanium oxide and its composite showed polycrystalline nature. SEM results elucidated that the incorporation of Titanium oxide into zeolite changed the surface morphology from rectangular to spherical. Ultraviolet visible spectroscopy shows that the bandgap of zeolite, titanium oxide, and its composite is 3.4, 3.2, and 4.14 eV, respectively. Current voltage results confirmed the formation of p-n heterojunction formed between p- and n-type materials indicating the behavior of solar cell devices.

Keywords: Composite; SEM; Synthesis; Titanium Oxide; Zeolite.

How to cite this article

Singh Dandolia R., Singh Tomar Sh., Dandotia A., Tomar R., Tiwari R.K. Synthesis and characterization of Titanium Dioxide modified zeolite-x based composite: To study the solar cell application. *Int. J. Nano Dimens.*, 2022; 13(4): 344-352.

INTRODUCTION

Dye-sensitized solar cells (DSSCs) are relatively new and promising photovoltaic technologies due to their simple and inexpensive manufacturing technology and various applications [1-3]. DSSCs have improved their power conversion efficiency (PCE) and stability throughout time, with the highest PCE today reaching 14.3 percent [4-5]. A photoelectrode, a dye, an electrolyte, and a counter electrode make up standard DSSCs. The PCE is highly dependent on the electron transfer "efficiency" at various photoelectrode (PE)/dye/electrolyte/counter electrode (CE) interfaces, as well as the electron transport "efficiency" at various cell components (PE, electrolyte, CE) and the photoelectrode's current collection capabilities [6-7]. As a result, photoelectrode

materials are critical for the future development of DSSCs, particularly in terms of light absorption and electron transport. This type of solar cell is thought to be a promising a third generation, due to its compatibility with solar energy devices flexible substrates high conversion efficiency that is practical. Indoor visible light with a positive reaction and the utilization of industrial waste are both possibilities [8-11]. Although these cells are showing the highest conversion efficiency reported so far is around 11% [12]. Even have though it fits the requirements of a wide range of practical applications [13-14]. In comparison to silicon solar cells, it is regarded as low DSSC is a photo-electrochemical system in which the photoanode is a porous nanostructured oxide layer. Dye molecules are adsorbed on the surface of nanostructured oxide sheets to boost

* Corresponding Author Email: r.k.dandolia@gmail.com

the photoanode's light absorption capability. Nanoparticle-based films are the most frequently utilized nanostructures so far due to their good light-collecting capability, high specific surface area, and ease of fabrication. Nanoparticles may be easily manufactured using a simple wet chemical technique, and film formation, such as using a doctor blade, will become easier. Even though nanoparticle-based films have a high surface area, the multiple barriers present in the nanoparticles network would obstruct photo-generated electron transport, lowering the energy conversion efficiency. The working electrode, photoanode, dye, electrolyte, catalyst, and the counter electrode are the major components of DSSCs in a photoconversion device. Because it intermediates the absorption of smaller or greater amounts of the dye, which is responsible for light absorption, the photoanode is an important component in the DSSC cell architecture. A considerable amount of dye enables better absorption and, as a result, an overall increase in cell conversion efficiency. To date, various photoanode materials have been investigated [15-18].

TiO₂ has been identified as a viable electrode material for DSSCs due to its large band gaps, which allows interfacial electron transport [19–21]. In DSSCs, the functional ingredient responsible for light absorption (the dye) is segregated from the charge carrier transport channel, unlike in conventional cells. Based on the realistic energy-conversion efficiency, this allows low-to-medium purity materials to be employed in a low-cost process, whereas the materials used in DSSCs are ecologically favorable [22]. Furthermore, for the development of high-efficiency DSSCs, an understanding of photoexcited electron kinetics in the photo-electrochemical cell throughout its operation is critical [23-24]. A titanium oxide semiconductor is widely used as a photoanode because of its unique properties like electrical, optical, and chemical with high conversion efficiency but its low detection and fast reverse electron transfer rate. Therefore, Alwan and Ali have modified TiO₂ and obtained better results for DSSC. Further, many scientists thought about new alternative photoanode materials for better performance of Dye-sensitized solar cells [25-30]. On the other hand, this problem can be overcome by introducing zeolite mesoporous material. Among them, Zeolites are crystalline aluminosilicates with molecular-sized holes and

channels. Interconnected aluminosilicate building components, such as SiO₄ or AlO₄ tetrahedra, joined by sharing oxygen atoms to form three-dimensional frameworks. Zeolite provides a large surface area and many other properties. Zeolite has many unique properties such as ion exchange, chemical and physical properties and pore size, and large surface area. This is the cheapest and easy synthesis material. This type of material is absorbed light in a large wavelength range of 300–800 nm. Therefore, the amount of zeolite added to the photoanode plays a major role [31-33]. It has been reported that zeolites in conjunction with metal oxide semiconductors such as zeolites can be used as a host for metal oxide nanostructure in a variety of applications like solar cell applications.

In this work, inclusion of TiO₂ into zeolite framework composites for the fabrication of dye-sensitized solar cells (DSSCs) is reported. But this study is mainly focused on the as-synthesized zeolite material with titanium oxide composite with absorbing ruthenium dye (N719) for improved results of I-V characteristics. Hydrothermal techniques were used to successfully produce zeolite and titanium oxide particles, and sol-gel techniques were used to create the composite. The doctor blade technique was used to apply the prepared powder composites to the FTO substrate. This substrate is also used for sensitization dye as a prepared photoanode and checked I-V performance was evaluated for solar cell applications.

EXPERIMENT

Materials

Fluorine tin oxide (FTO) conducting glass slides were purchased from Merck, Sodium Hydroxide (NaOH), acetone (C₃H₆O), ethanol (C₂H₅OH), and acetic acid (CH₃CO₂H), Titanium Tetraisopropoxide (TTIP), isopropyl alcohol (IPA) were purchased from Sigma-Aldrich (St. Louis, MS, USA) and were used without further purification.

Synthesis of zeolite -X

25 g of sodium hydroxide was dissolved in 25 ml of distilled water. To the sodium hydroxide solution, 24.25 g of alumina trihydrate was added and stirred at 100°C until dissolved. The solution was cooled to 25 °C, and 50.5 ml of water was added to the mixture. This solution is named 'A'. To 25 ml of solution 'A', 153 ml of water and 14.78 g of sodium hydroxide were added. This

solution is named 'B'. In a separate beaker, 54.5 ml of a sodium silicate solution, 153 ml of water, and 14.78 g of sodium hydroxide were mixed until complete dissolution. This solution was labelled as 'C'. Solutions 'B' and 'C' were mixed quickly and stirred for 30 minutes. After 30 minutes the final solution was poured into a polyethylene bottle and kept in an oven at 90 °C for 8 hours for crystallization. The formed Zeolite Na-X was washed and dried at 100 °C.

Preparation of composite

We prepare zeolite and TiO₂ composites as follows. First taken 1 g of zeolite, 1.6 ml of TTIP and 4.33 ml of IPA were mixed well at 60 °C for 1 hour using a magnetic stirrer. After this process, add 23.33 ml of deionized water and 10 ml of IPA, then stirrer at the same temperature for an additional 2 hours. The resulting sample is then dried at 60 °C for 4 hours.

Preparation of Photoanode

The photoanodes or working electrodes were fabricated by the doctor blade method. The titanium dioxide paste was prepared by adding desired amounts of binder, and Zeolite/TiO₂ powder taken in a mortar and pestle and it was ground. Few drops of Acetylacetone and Polyethylene glycol were further added to the mixture and it was ground. This paste is used for making a layer on the FTO substrate. Before utilization, FTO glasses substrates were washed and cleaned.

FTO substrates were first cleaned in an ultrasonic water bath using deionized water, ethanol, and acetone respectively for each of 10 minutes.

The required amount of Zeolite/TiO₂ paste was coated on an unmasked area and uniformly spread over the FTO substrate using glass rod as a doctor blade technique. The layered FTO glass substrate was leftover for 10 min without touching the surface and tapes were carefully removed. This substrate was put in an oven for annealed at 500°C and then cooled down at room temperature. This substrate was obtained as a colour white surface. The calcination process provides all the solvents removed from the surface of the substrate. After that the process of sensitization of photoanode requires the film to be soaked inside the dye solution for one day. Further, this FTO substrate was washed via ethanol for removing unsoaked

dye molecules from the surface and counter electrodes is prepared and both substrates put together like sandwich. Then I-V performance of this solar cell was checked by using Potentiostat instruments (Autolab-PSTAT-204).

Characterization

The structural property of as-prepared Zeolite, Titanium oxide, and its composite was characterized using an X-ray diffractometer, RIGAKU Miniflex-600 with Cu-K α source ($\lambda=1.5405\text{\AA}$) radiation. The surface morphology of the material was characterized using a Scanning electron microscope (Philips, Model-Quanta 200 FEG). UV-Vis optical transmittance of prepared material was carried out using a Shimadzu-UV-2450 spectrophotometer. The I-V characteristics of the solar cells were tested using a computer-controlled Potentiostat (Autolab-PSTAT-204) with a 50 W Halogen Lamp under condition.

RESULT & DISCUSSION

XRD Analysis

The powder X-Ray Diffraction pattern of synthesized zeolites, TiO₂, and their composite as shown in Fig. 1 were recorded by using a Mini Flex 600 X-ray powder diffractometer (XRD) with a scan rate of 2° to 90°. From Fig. 1, it is seen that all samples show a highly crystalline nature but their composite shows slight amorphous phases. Also, it is found that there is minimal variation, particularly in the intensity of peaks in all samples. The synthesis of zeolite particles has been verified [34]. The crystal structure of the hydrothermally produced TiO₂ was discovered to be anatase phase based on the XRD pattern. It was also discovered to be a good match for JCPDS card No. 21-1272 [35]. The X-ray diffraction patterns of TiO₂ samples show a tetragonal crystal structure, with diffraction peaks indexed to the (101), (112), (200), (105), (211), (204), (116), and (220) lattice planes with Bragg diffraction angles (2 θ) of 25.26°, 37.93°, 48.18°, 54.06°, 55.13°, 62.85° respectively.

The Scherrer equation (1) was used to calculate the average crystalline size, and the results are shown in Table 1.

$$D = \frac{k}{\beta \cos \theta} \quad (1)$$

Where, D is the average crystalline size, k = 0.9 (Scherrer constant), λ is the X-ray source wavelength (0.15406 nm), β is the full width at half

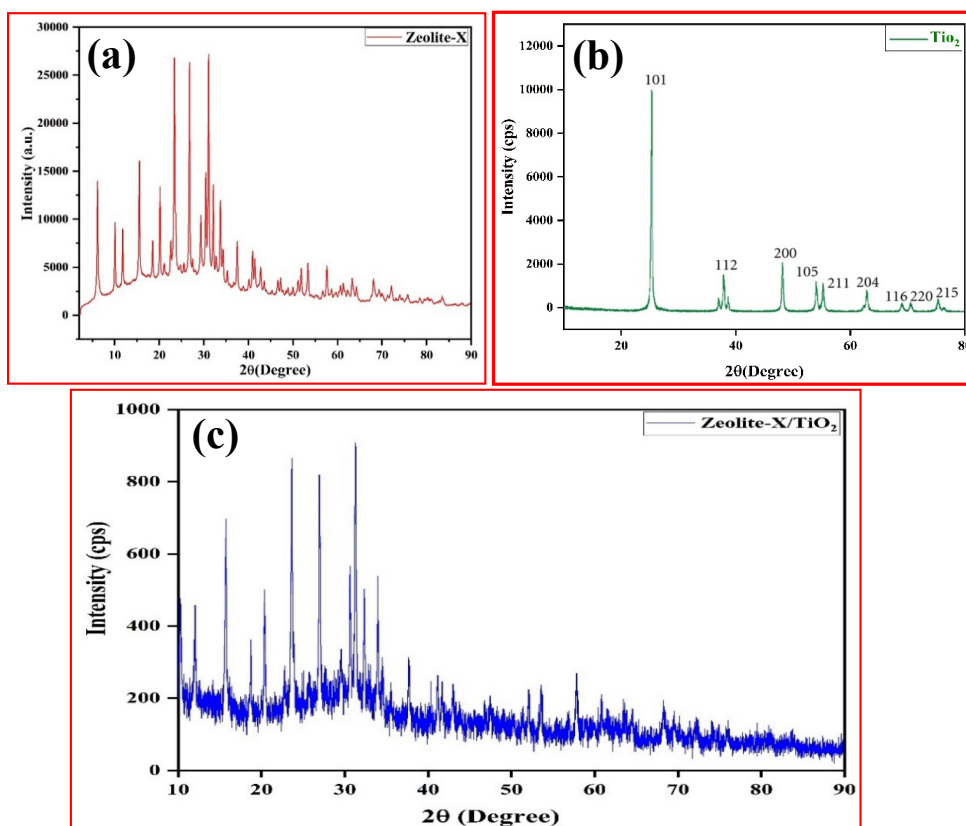


Fig. 1. XRD pattern of (a) Zeolite-X, (b) TiO₂ and (c) Zeolite/TiO₂ Composite.

Table 1. The crystalline size of samples.

NPs	Crystalline size (nm)
Zeolite-X	53.19
TiO ₂	55.7
Composite	58.4

maximum (FWHM) value, and θ is the diffraction Bragg angle.

SEM Analysis

The surface morphology of synthetic zeolite, TiO₂, and their composites is characterized by SEM micrograph analysis as shown in Fig. 2. The synthesized zeolite particles have a polyhedrons shape with having particle size in 1-3 micro metre. The typical particle size of TiO₂ nanoparticles is less than 0.1 micrometre, according to SEM data. SEM pictures of zeolite-supported TiO₂ revealed a consistent distribution of spherical nanoparticles on the solid support's surface.

Optical Properties

The absorption characteristic of Zeolite, Titanium oxide, and its composite was determined using UV-Vis spectroscopy. The bandgap of as-prepared material was calculated using the tauc relation. The absorption spectra of Zeolite, Titanium oxide, and its composite and associated Tauc plot are shown in Fig. 3 (a-f).

The equation [36] gives the tauc relation as below

$$ah\nu = A(h\nu - E_g)^n \quad (2)$$

Where, A is the proportionality constant, a is

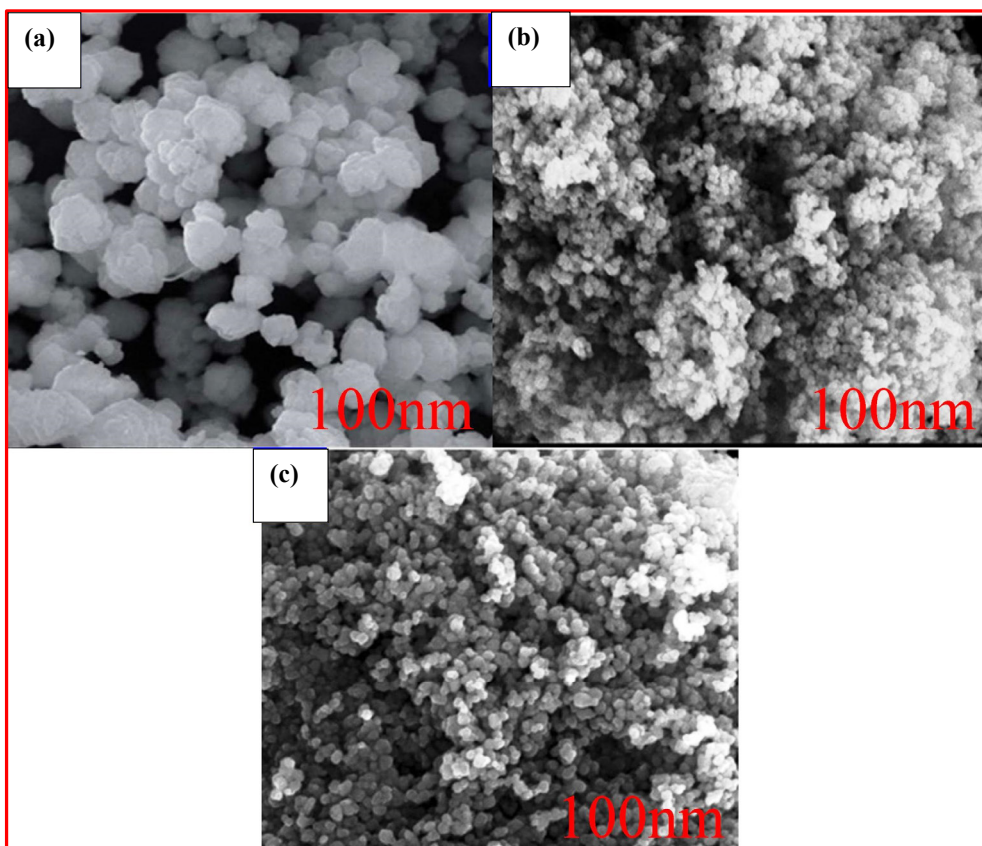


Fig. 2. SEM micrographs of (a) Zeolite-X, (b) TiO_2 , and (c) Zeolite/ TiO_2 composite.

the absorption coefficient, h is Planck's constant, u is the light frequency, n is $1/2$ for direct band transition, and E_g is the bandgap.

Extrapolating the linear portion of the graph between $(\alpha h\nu)^2$ versus $h\nu$ yields the bandgap values. The bandgap is determined by the intersection of the tangent line with the x-axis. The results obtained demonstrates the Zeolite, Titanium oxide, and its composite straight bandgap feature, with a bandgap value of roughly 3.4, 3.2, and 4.14 eV respectively, which is acceptable for solar cells.

Electrochemical Impedance Spectroscopy (EIS) Analysis

The charge carriers transport characteristics and capacitance of photovoltaic devices were investigated using electrochemical impedance spectroscopy (EIS) in the dark at 0.1 V applied bias with frequencies ranging from 1 Hz to 1 MHz. The results of Nyquist plots can be fitted with a corresponding circuit incorporating series

resistance (R_s), recombination resistance (R_{rec}), and capacitance (C), which are essential factors in determining solar cell performance. The device's recombination resistance should be as high as feasible, allowing charge carriers to accumulate in the capacitor element to flow via the external circuit, and a large capacitance value determines the device's charge storing ability [37-38].

Fig. 4 shows the Nyquist plot (1 Hz to 1 MHz) in dark and light conditions when the manufacturing equipment is biased. Z_w is Warburg impedance related to the diffusion process of charge carriers at the interface. A steeper slope in the mid-frequency region of the Nyquist plot could be attributed to the Warburg behavior caused by fast diffusion. From the Nyquist plot, the values of R_s , R_p , and CPE were found to be 102 Ω , 886.8 Ω , and 23.9 μF , respectively.

Current-Voltage Characteristics Analysis

Fig. 5 shows the Current-Voltage characteristics of the device carried out under dark and light

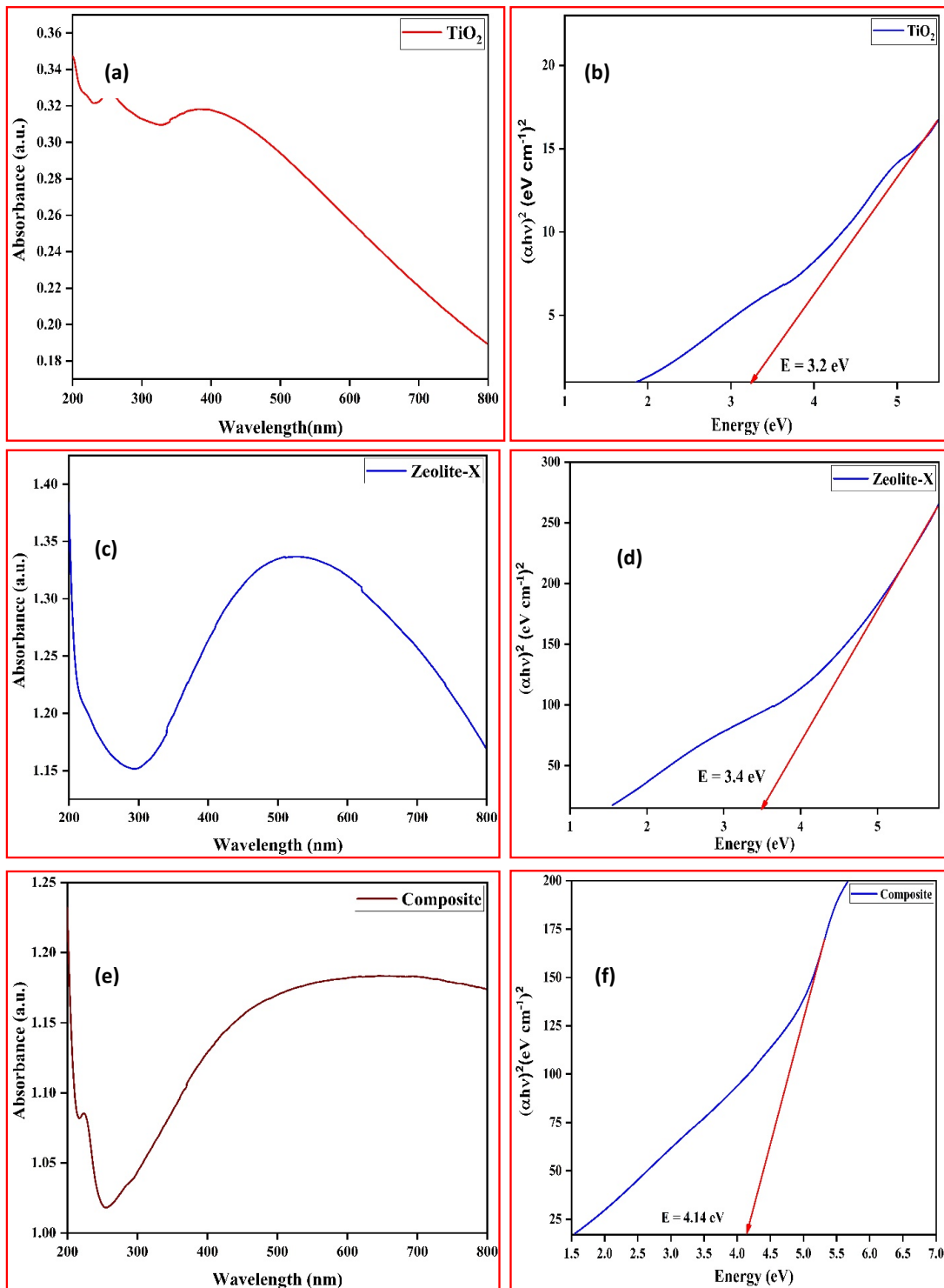


Fig. 3. Optical absorbance spectra and Tauc plots of (a-b) TiO₂, (c-d) Zeolite-X, and (e-f) Zeolite/TiO₂ composite.

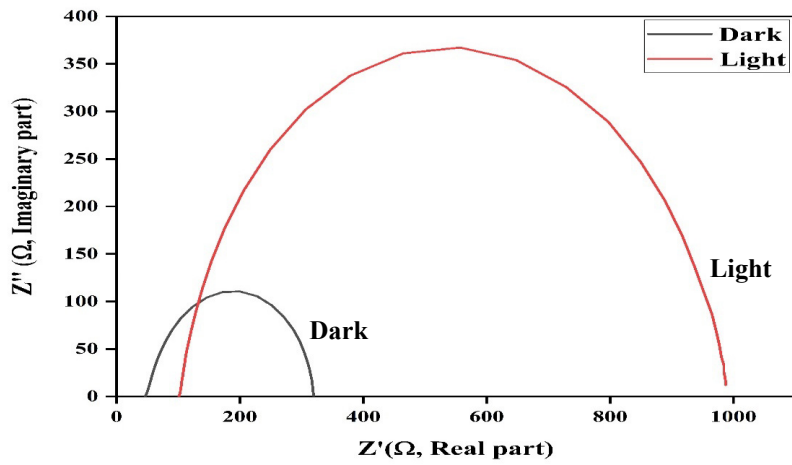


Fig. 4. Nyquist plots of solar cells with and without light.

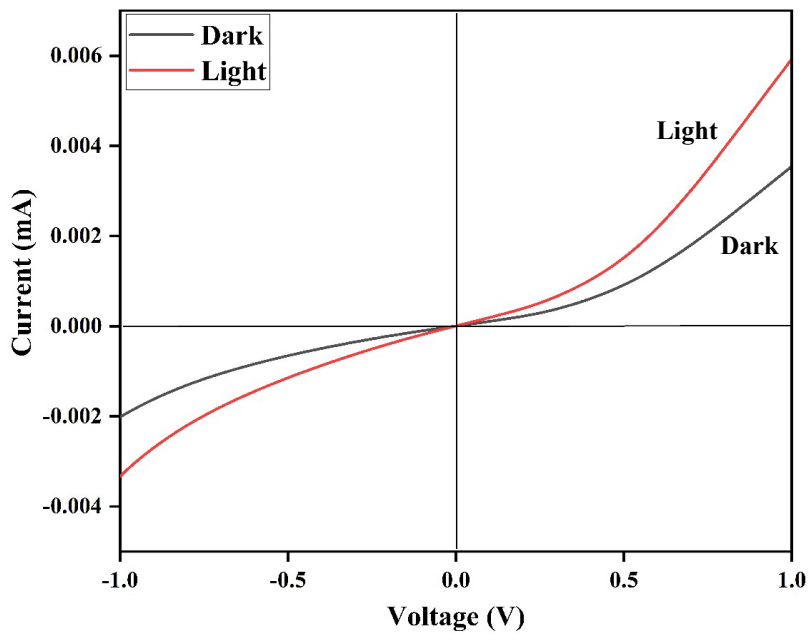


Fig. 5. Current-Voltages characteristics of the device.

(halogen lamp light source of 50 W). Current-Voltages results revealed that a p-n heterojunction is formed with rectifying behavior of the fabrication device. The results also showed that a created p-n junction diode is light sensitive. Therefore, it may be used as an Electron Transfer layer (ETLs)/Hole Transfer Layer (HTLs) as solar cells and photodiodes applications.

CONCLUSION

To summarise, we have successfully synthesized zeolite-X and Titanium oxide by using a hydrothermal method, and its composite was prepared by the sol-gel method. The synthesized materials were characterized by different techniques such as XRD, FTIR, SEM, and UV-Vis spectroscopy analysis. X-Ray Diffraction analysis

confirmed the polycrystalline nature of the material. Fourier transform infrared spectroscopy analysis show the vibrational frequencies of the bonds in synthesis material. Scanning electron microscopy Analysis shows the morphology of the sample. Ultraviolet-Visible Spectroscopy analysis shows that the bandgap of the sample is 3.4, 3.2, and 4.14 eV, respectively. From the Nyquist plot, the values of R_s , R_p , and CPE were found to be 102 Ω , 885.8 Ω , and 23.9 μF , respectively. I-V results confirmed the formation of p-n heterojunction was formed between p- and n-type materials indicating that this is the behavior of solar cell devices. Our results strongly confirmed improvement in solar cells to enhance efficiency by changing the light source and interface.

ACKNOWLEDGMENTS

The authors are very thankful to IIC-IIT Roorkee, for providing the SEM facilities. We also very thankful to the CIF, Jiwaji University, Gwalior and Panjab University, for extending the, XRD, FTIR, and optical facilities respectively.

AUTHOR CONTRIBUTIONS

R. K. S. D carried out the synthesis and wrote the manuscript. A. D. did the plot the figure and helped in writing the manuscript. S. S. T. and R.K. T. helped in discussion and analysis of the results in the manuscript.

COMPETING INTERESTS

The authors declare no competing interests.

ETHICS APPROVAL

Not applicable

CONSENT TO PARTICIPATE

Not applicable

CONSENT FOR PUBLICATION

Not applicable

AVAILABILITY OF DATA

This data always available on corresponding email id.

MATERIAL FUNDING

No

REFERENCES

[1] Ahmad M. S., Pandey A. K., Abd Rahim N., (2017),

Advancements in the development of TiO_2 photoanodes and its fabrication methods for dye sensitized solar cell (DSSC) applications. A review. *Renew. Sust. Energ. Rev.* 77: 89-108.

- [2] So S., Hwang I., Schmuki P., (2015), Hierarchical DSSC structures based on "single walled" TiO_2 nanotube arrays reach a back-side illumination solar light conversion efficiency of 8%. *Energy Environ. Sci.* 8: 849-854.
- [3] John K. A., Naduvath J., Remillard S. K., Shaji S., DeYoung P. A., Kellner Z. T., Philip R. R., (2019), A simple method to fabricate metal doped TiO_2 nanotubes. *Chem. Phys.* 523: 198-204.
- [4] Xie K., Guo M., Liu X., Huang H., (2015), Enhanced efficiencies in thin and semi-transparent dye-sensitized solar cells under low photon flux conditions using TiO_2 nanotube photonic crystal. *J. Power Sources.* 293: 170-177.
- [5] Wang H., Liu Q., Liu D., Su R., Liu J., Li Y., (2018), Computational prediction of electronic and photovoltaic properties of anthracene-based organic dyes for dye-sensitized solar cells. *Int. J. Photoenergy.* 2018: Article ID: 4764830.
- [6] Halme J., Vahermaa P., Miettunen K., Lund P., (2010), Device physics of dye solar cells. *Adv. Mat.* 22: E210-E234.
- [7] Tsvetkov N., Larina L., Ku Kang J., Shevaleevskiy O., (2020), Sol-gel processed TiO_2 nanotube photoelectrodes for dye-sensitized solar cells with enhanced photovoltaic performance. *Nanomater.* 10: 296-302.
- [8] O'regan B., Grätzel M., (1991), A low-cost, high-efficiency solar cell based on dye-sensitized colloidal TiO_2 films. *Nature.* 353: 737-740.
- [9] Yahya M., Bouziani A., Ocak C., Seferoğlu Z., Sillanpää M., (2021), Organic/metal-organic photosensitizers for dye-sensitized solar cells (DSSC): Recent developments, new trends, and future perceptions. *Dyes Pigm.* 192: 109227.
- [10] Yu J., Fan J., Lv K., (2010), Anatase TiO_2 nanosheets with exposed (001) facets: Improved photoelectric conversion efficiency in dye-sensitized solar cells. *Nanoscale.* 2: 2144-2149.
- [11] Hafez H., Lan Z., Li Q., Wu J., (2010), High efficiency dye-sensitized solar cell based on novel TiO_2 nanorod/nanoparticle bilayer electrode. *Nanotechnol. Sci. Appl.* 3: 45-49.
- [12] Nazeeruddin M. K., Kay A., Rodicio I., Humphry-Baker R., Müller E., Liska P., Grätzel M., (1993), Conversion of light to electricity by cis- X_2 bis (2, 2'-bipyridyl-4, 4'-dicarboxylate) Ruthenium (II) charge-transfer sensitizers (X= Cl-, Br-, I-, CN-, and SCN-) on nanocrystalline titanium dioxide electrodes. *J. Am. Chem. Soc.* 115: 6382-6390.
- [13] Mora-Sero I., Giménez S., Fabregat-Santiago F., Gómez R., Shen Q., Toyoda T., Bisquert J., (2009), Recombination in quantum dot sensitized solar cells. *Acc. Chem. Res.* 42: 1848-1857.
- [14] Grätzel M., (2005), Solar energy conversion by dye-sensitized photovoltaic cells. *Inorg. Chem.* 44: 6841-6851.
- [15] Yildiz Z. K., Atilgan A., Atli A., Özel K., Altinkaya C., Yildiz A., (2019), Enhancement of efficiency of natural and organic dye sensitized solar cells using thin film TiO_2 photoanodes fabricated by spin-coating. *J. Photochem. Photobiol. A.* 368: 23-29.
- [16] Gnida P., Jarka P., Chulkin P., Drygała A., Libera M., Tański T., Schab-Balcerzak E., (2021), Impact of TiO_2 nanostructures on dye-sensitized solar cells performance. *Mater.* 14: 1633-1637.

- [17] Kathirvel S., Chen H. S., Su C., Wang H. H., Li C. Y., Li W. R., (2013), Preparation of smooth surface TiO₂ photoanode for high energy conversion efficiency in dye-sensitized solar cells. *J. Nanomater.* 2013: Article ID 367510.
- [18] Tsai J. K., Hsu W. D., Wu T. C., Meen T. H., Chong W. J., (2013), Effect of compressed TiO₂ nanoparticle thin film thickness on the performance of dye-sensitized solar cells. *Nanoscale Res. Lett.* 8: 1-6.
- [19] Tong Z., Peng T., Sun W., Liu W., Guo S., Zhao X. Z., (2014), Introducing an intermediate band into dye-sensitized solar cells by W6+ doping into TiO₂ nanocrystalline photoanodes. *The J. Phys. C.* 118: 16892-16895.
- [20] Kakiage K., Aoyama Y., Yano T., Otsuka T., Kyomen T., Unno M., Hanaya M., (2014), An achievement of over 12 percent efficiency in an organic dye-sensitized solar cell. *Chem. Comm.* 50: 6379-6381.
- [21] Graetzel M., Janssen R. A., Mitzi D. B., Sargent E. H., (2012), Materials interface engineering for solution-processed photovoltaics. *Nature.* 488: 304-312.
- [22] Mariotti N., Bonomo M., Fagiolari L., Barbero N., Gerbaldi C., Bella F., Barolo C., (2020), Recent advances in eco-friendly and cost-effective materials towards sustainable dye-sensitized solar cells. *Green Chem.* 22: 7168-7218.
- [23] Yeoh M. E., Chan K. Y., (2017), Recent advances in photoanode for dye-sensitized solar cells: A review. *Int. J. Energy Res.* 41: 2446-2467.
- [24] Scarabino S., Nonomura K., Vlachopoulos N., Högfeldt A., Wittstock G., (2020), Effect of TiO₂ photoanodes morphology and dye structure on dye-regeneration kinetics investigated by scanning electrochemical microscopy. *Electrochem.* 1: 329-343.
- [25] Leung D. Y., Fu X., Wang C., Ni M., Leung M. K., Wang X., Fu X., (2010), Hydrogen production over titania-based photocatalysts. *Chem. Sus. Chem.* 3: 681-694.
- [26] Liu G., Gong J., Kong L., Schaller R. D., Hu Q., Liu Z., Xu T., (2018), Isothermal pressure-derived metastable states in 2D hybrid perovskites showing enduring bandgap narrowing. *Proc. Natl. Acad. Sci.* 115: 8076-8081.
- [27] Hutter E. M., Sutton R. J., Chandrashekar S., Abdi-Jalebi M., Stranks S. D., Snaith H. J., Savenije T. J., (2017), Vapour-deposited cesium lead iodide perovskites: Microsecond charge carrier lifetimes and enhanced photovoltaic performance. *ACS Energy Lett.* 2: 1901-1908.
- [28] Wang X., Li Z., Shi J., Yu Y., (2014), One-dimensional titanium dioxide nanomaterials: Nanowires, nanorods, and nanobelts. *Chem. Rev.* 114: 9346-9384.
- [29] Ooyama Y., Harima Y., (2012), Photophysical and electrochemical properties, and molecular structures of organic dyes for dye-sensitized solar cells. *Chem. Phys. Chem.* 13: 4032-4080.
- [30] Alfanaar R., Elim P. E., Yuniati Y., Kusuma H. S., Mahfud M., (2021), Synthesis of TiO₂/ZnO-anthocyanin hybrid material for dye sensitized solar cell (DSSC). *In IOP Conf. Series: Mater. Sci. and Eng.* 1053: 012088.
- [31] Cejka J., Van Bekkum H., Corma A., Schueth F., (2007), Introduction to zeolite molecular sieves. *Elsevier.*
- [32] Corma A., Zones S., Cejka J., (Eds.), (2010), Zeolites and catalysis: synthesis, reactions and applications. *John Wiley & Sons.*
- [33] Kulprathipanja S., (Ed.) (2010), Zeolites in industrial separation and catalysis. *John Wiley & Sons.*
- [34] Naikoo R. A., Bhat S. U., Mir M. A., Tomar R., Khanday W. A., Dipak P., Tiwari D. C., (2016), Polypyrrole and its composites with various cation exchanged forms of zeolite X and their role in sensitive detection of carbon monoxide. *RSC Adv.* 6: 99202-99210.
- [35] Li W., Liang R., Hu A., Huang Z., Zhou Y. N., (2014), Generation of oxygen vacancies in visible light activated one-dimensional iodine TiO₂ photocatalysts. *RSC Adv.* 4: 36959-36966.
- [36] Sun Y., Lei J., Wang Y., Tang Q., Kang C., (2020), Fabrication of a magnetic ternary ZnFe₂O₄/TiO₂/RGO Z-scheme system with efficient photocatalytic activity and easy recyclability. *RSC Adv.* 10: 17293-17301.
- [37] Back S., Kim J. H., Kim Y. T., Jung Y., (2016), Bifunctional interface of Au and Cu for improved CO₂ electroreduction. *ACS Appl. Mater. Interf.* 8: 23022-23027.
- [38] Rahman A., Nurjayadi M., Wartilah R., Kusri E., Prasetyanto E. A., Degermenci V., (2018), Enhanced activity of TiO₂/Natural zeolite composite for degradation of methyl orange under visible light irradiation. *Int. J. Technol.* 9: 1159-1167.